May, 1993] © *1993 The Chemical Society of Japan* *Bull. Chem. Soc. Jpn.*, ***66***, *1333—1342(1993)* 1333

Novel Organic Ions of High-Spin States. III. ESR and ^{1}H ENDOR Studies of a Monocation of *m*-Phenylenebis(phenylmethylene)

Michio MATSUSHITA, Toshihiro NAKAMURA, Takamasa MOMOSE, Tadamasa SHIDA,* Yoshio TEKI,† Takeji TAKUI,† Takamasa KINOSHITA,† and Koichi ITOH*,†
Department of Chemistry, Faculty of Science, Kyoto University, Kyoto 606-01
†Department of Chemistry, Faculty of Science, Osaka City University, Sugimoto, Sumiyoshi-ku, Osaka 558

(Received November 2, 1992)

The monocation of *m*-phenylenebis (phenylmethylene)(*m*-PBPM), the first high-spin hydrocarbon cation, has been generated by γ-radiolysis and subsequent photolysis of 1,3-bis(α-diazobenzyl)benzene in *s*-butyl chloride at 77 K. The system is studied by ESR and ^{1}H ENDOR spectroscopy. Two conformers of the monocation are detected which are associated with spin Hamiltonian parameters of $S=3/2$, $g=2.003$, $D=0.1350$ cm^{-1}, and $|E|=0.0040$ cm^{-1} and $S=3/2$, $g=2.003$, $D=0.1285$ cm^{-1}, and $|E|=0.0055$ cm^{-1}, respectively. The off-axis extra lines characteristic of the quartet-state powder pattern ESR spectra were identified. The ground state of both the cations is confirmed to be spin-quartet by the measurement of their ESR intensity at low temperatures. The ^{1}H ENDOR measurement has shown that the electron in the nonbonding π-orbital is removed upon ionization to yield the π-cation. The hyperfine structure due to the divalent ^{13}C was found to be consistent with the electronic structure of the π-cation. A semiempirical calculation of the fine structure parameters D and E has been carried out in terms of spin–spin interaction. The semiempirical calculation and the electronic structure suggest that both the cations are in a trans–trans conformation in contrast to a cis–trans for the neutral *m*-PBPM. The result is discussed in comparison with the monoanion of *m*-PBPM.

Organic high-spin molecules[1—7] (whose molecular spin quantum number S in their ground state is larger than unity) have been accepting wide and increasing interests both experimentally and theoretically. The high-spin molecules are not only suitable model systems for organic/molecular based ferro- and superparamagnets but also important in spin chemistry. The purpose of studying the high-spin molecules is numerous including i) the understanding of both intra- and intermolecular spin alignment in organic systems, ii) the exploration of the possibility of spin quantum mixing of high-spin organic systems, iii) the test for the validity of MO and VB theories in various levels and the construction of theories capable enough to predict the spin state, iv) the designing of organic/molecular high-spin assemblages and their spin control at will. Spin chemistry is finding ever increasing applications in molecular engineering of organic/molecular based magnetic materials. The search for these materials is rigorous in both pure and applied sciences.[8—10]

Among increasing subjects in spin chemistry, charged organic high-spin systems have attracted particular attention not only because of their novelty but also because of their suitability as a model for clarifing an important issue of spin vs. charge fluctuation in organic molecules. This is crucial for developing new materials such as organomagnetic metal.

Recently we have detected and characterized the first charged high-spin hydrocarbon molecule, that is, the monoanion of *m*-phenylenebis(phenylmethylene) (*m*-PBPM).[11,12] As for the neutral polycarbenes such as *m*-PBPM, the spin alignment is dictated by the topology of the π-electron network,[1—4,13—19] as has been shown repeatedly by the Osaka group.[5,20—26] Basic and extensive studies of neutral molecular based magnetism in terms of spin chemistry have been reported by other groups also.[6—10,27—48] In contrast, only a qualitatively prediction was made for the spin alignment when neutral high-spin molecules are ionized, according to which the order of high and low-spin states may be reversed upon the charging of parent neutral molecules.[49,50] Our recent experimental study of the high-spin monoanion has shown that more elaborate theoretical treatments are definitely required for the prediction of the spin state of charged systems. Under the circumstance it is desirable to accumulate experimental data on the charged system. Thus, in addition to the high-spin monoanion of *m*-PBPM, we have generated and characterized the monocation of *m*-PBPM, which is the first cation of high-spin hydrocarbon molecules. Optical, ESR, and ^{1}H ENDOR spectroscopic studies have been carried out to see the effect of the electron removal upon the spin alignment.

Experimental

1,3-Bis(α-diazobenzyl)benzene(1,3-BDB), which is the precursor of *m*-PBPM, was synthesized by a standard method in the literature.[51,52] It was dissolved in *s*-butyl chloride(BuCl) to a concentration of 5—10 mM (1 M=1 mol dm^{-3}) and sealed off in ESR or optical cells after degassing. The solution frozen at 77 K was γ-irradiated by ^{60}Co to a dose of ca. 1.6 kGy (1 Gy=1 J kg^{-1}). This procedure leads to the formation of the doublet radical cation of the solute, 1,3-BDB, as has been described elsewhere[53—55] (see the next section). The cation was, then, photolized to yield the cation of *m*-PBPM at cryogenic temperatures. The photolysis effects the elimination of nitrogen from the doublet radical cation of 1,3-BDB to generate the cation of *m*-PBPM. It should be noted that this procedure involves the spin conversion from the doublet of the radical cation of 1,3-BDB to the high-spin cation of *m*-PBPM if the cation of *m*-PBPM is high-spin (quartet) in the ground state. The ^{13}C-labeled diazo precursor, 1-(α-diazobenzyl)-3-(α-diazobenzyl-α-^{13}C)benzene was prepared as in the previous work on the monoanion of *m*-PBPM.$^{12)}$ The ESR measurement was performed with a JEOL PE-2X spectrometer equipped with an Air Products LTR-3 refrigerator and a Bruker ESP 300 spectrometer with an Oxford ESR 910 He gas-flow temperature controller. A Cary 17I spectrophotometer was used for the optical measurement. A Ushio halogen lamp (1000 W) with Toshiba cut-off glass filters, R-62, O-55, and Y-51, was used for the photolysis. The ^{1}H ENDOR measurement was performed with a Bruker ESP300/350 spectrometer with the Oxford ESR 910 temperature controller.

Results and Discussion

Optical and ESR Spectra. The solution of 1,3-BDB in BuCl becomes a glassy solid in purple at 77 K (see curve 1 in Fig. 1). The color is ascribable to the $n\pi^*$-transition of the diazo compound with $\varepsilon=254$ at $\lambda_{\max}=530$ nm.$^{56)}$ From the value of ε, we can estimate the concentration of the dissolved 1,3-BDB as 5—10 mM.

The major processes in the γ-irradiated BuCl glass can be summarized as in the following.$^{53—55)}$

$$\mathrm{BuCl} \xrightarrow{\gamma} \mathrm{BuCl}^{+\bullet} + \mathrm{e}^-, \qquad (1)$$

$$\mathrm{e}^- + \mathrm{BuCl} \rightarrow \mathrm{Bu}^{\bullet} + \mathrm{Cl}^-, \qquad (2)$$

$$\mathrm{BuCl}^{+\bullet} + \mathrm{BuCl} \rightarrow \mathrm{BuCl} + \mathrm{BuCl}^{+\bullet} \xrightarrow{\mathrm{S}} \mathrm{S}^{+\bullet} + \mathrm{BuCl}. \qquad (3)$$

Reaction (3) represents the positive charge transfer from the ionized BuCl to the solute 1,3-BDB, denoted by S. It should be emphasized that high-energy γ photons do not cause violent radiolysis to extensive fragmentations of the solvent and the solute but result mostly in thermal ionization of the solute by the intermolecular charge transfer as represented in reaction (3). The possibility of formation of dications is ignorable because of the Coulombic repulsion between two positive charges. As a result, the major products of the reactions are the butyl radical, the chloride anion, and the radical cation of 1,3-BDB, 1,3-BDB$^{+\bullet}$.$^{53—55)}$ The electronic absorption spectrum at this stage is shown in curve 2 of Fig. 1. Since the butyl radical and the chloride anion are colorless in the observed region, the spectrum in curve 2 is attributed to the radical cation of 1,3-BDB, although part of the $n\pi^*$-transition due to the intact 1,3-BDB (curve 1) is superposed. The absorption spectrum in curve 2 has a characteristic peak at 630 nm in contrast to the spectrum of γ-irradiated 1,3-BDB in a 2-methyltetrahydrofuran (MTHF) glass, which exhibits strong absorption at $\lambda<500$ nm and feeble absorption in the near-IR region (see curve 2 in Fig. 1 of Ref. 11). The difference between the two spectra clearly indicates that the species produced by γ-irradiation in BuCl, to be attributed to 1,3-BDB$^{+\bullet}$, is different from that in MTHF which has been attributed to the radical anion of 1,3-BDB.$^{11,12)}$ Further confirmation of the assignment of 1,3-BDB$^{+\bullet}$ was made by running a parallel optical study of a solution of 1,3-BDB (ca. 10 mM) plus triethylamine (TEA, ca. 100 mM) in BuCl; since TEA is known to be an efficient positive charge scavenger,$^{53—55)}$ the yield of the absorption in curve 2 of Fig. 1 should be suppressed drastically, which was indeed observed.

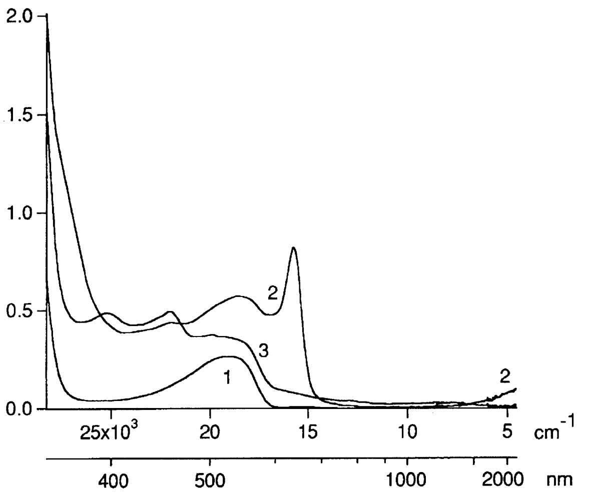

Fig. 1. Optical absorption spectra of 1,3-BDB/BuCl solution at 77 K: 1, before γ-irradiation; 2, after γ-irradiation; 3, same as 2 but followed by photolysis with $\lambda>550$ nm.

The X-band ESR spectrum after γ-irradiation was observed in the range of 0.32—0.34 T (1 T=Wb m^{-2}) as shown in the inset of Fig. 2, which is consistent with the formation of the spin-doublet 1,3-BDB$^{+\bullet}$ and the butyl radical by reactions (2) and (3).

When the γ-irradiated sample exhibiting the optical spectrum in curve 2 of Fig. 1 was photolyzed with $\lambda>$ 620 nm, several new ESR signals appeared in the wide range of the magnetic field 0—0.6 T (see Fig. 2). Concomitantly, the optical spectrum changed from curve 2 to 3 as seen in Fig. 1. The appearance of the new ESR signals indicates the formation of new high-spin species. Since these signals did not appear in the experiment of the 1,3-BDB+TEA/BuCl system, the new signals are associated with high-spin species originating from the radical cation of 1,3-BDB. By analogy with the photolytic denitrogenation of the parent 1,3-BDB molecule,$^{5)}$ the observed spectral change is accounted for by the following series of reaction.

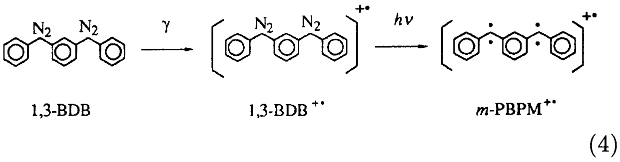

(4)

Since reactions (1) and (3) should lead solely to the

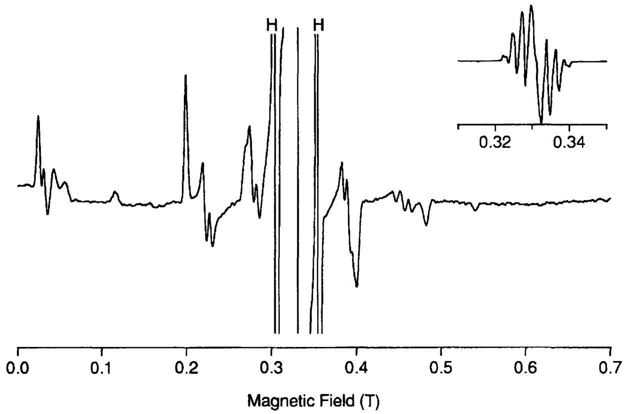

Fig. 2. X-Band ESR spectra for a γ-irradiated and subsequently photolyzed 1,3-BDB/BuCl solution at 36 K. Prior to photolysis only the signal was observed at 0.32—0.34 T, which is shown in the inset, and the doublet due to the hydrogen atom produced in the quartz cell by γ-irradiation. Upon photolysis several new peaks appeared in the ESR spectrum over a wide range of 0—0.6 T. The new peaks are assigned to the spin quartet state of m-PBPM$^{+\bullet}$.

monocation of 1,3-BDB, and since the photon energy in reaction (4) is less than ca. 2 eV, there is no possible occurrence of photoionization to the dications of 1,3-BDB or m-PBPM in reaction (4). Since only the doublet or the quartet is allowed for the spin multiplicity of m-PBPM$^{+\bullet}$, the fine structure observed at 0—0.6 T must be referred to m-PBPM$^{+\bullet}$ in its quartet state. The accompanying optical change from curve 2 to 3 in Fig. 1 is, thus, attributed to the formation of quartet m-PBPM$^{+\bullet}$. The ESR spectrum in Fig. 2 resembles that of the monoanion of m-PBPM. The resemblance will be accounted for consistently by invoking the pairing theorem of conjugated π-electron systems.[57—59] A closer analysis of the observed ESR spectrum in Fig. 2 reveals that there are two conformers of quartet m-PBPM$^{+\bullet}$ as will be discussed in the following section.

Analysis of the X-Band ESR Spectra: Appearance of the Off-Axis Extra Line of the Quartet State. As in the previous work on the monoanion of m-PBPM,[11] the ESR assignment was confirmed by the simulation based on the following spin Hamiltonian.

$$\mathscr{H} = g\beta\boldsymbol{S}\cdot\boldsymbol{H} + D[S_Z{}^2 - S(S+1)/3] + E(S_X{}^2 - S_Y{}^2), \quad (5)$$

where each term has the usual meaning and $S=3/2$. The Hamiltonian corresponding to a particular orientation of the magnetic field was diagonalized to obtain the resonant field and the transition probability. Then, the spectrum was summed up over the whole spherical angle of 4π to get the powder-pattern spectrum. On account of the symmetry of the fine-structure tensor, it is necessary to integrate only one eighth of the sphere. A total of 6500 orientations were sampled and a Gaussian line-width of 4.0 mT was assumed commonly to each ESR transition.

After several trials of the simulation we concluded that the observed spectrum is a superposition of two spin-quartet constituents having slightly different fine structure parameters. At the bottom of Fig. 3 are shown the constituent spectra and the spectrum in the middle is their superposition. In the superposed spectrum the low and the high-field pairs of the Y-axis

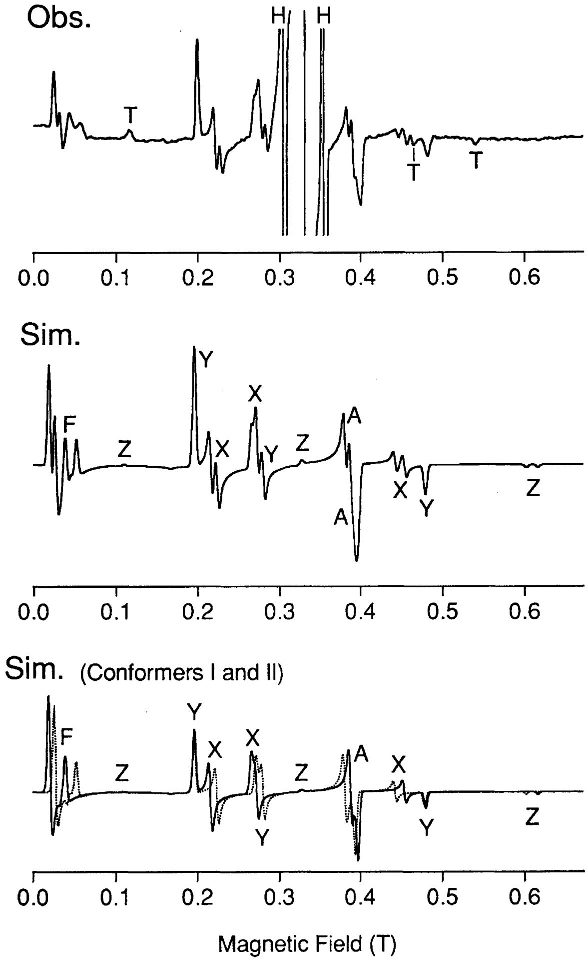

Fig. 3. Observed and simulated X-band ESR spectra for the quartet state of m-PBPM$^{+\bullet}$. The symbol T in the observed spectrum indicates the signals due to by-produced triplet carbenes. Microwave frequency employed was 9.175 GHz. Symbols A and F in the simulated spectra denote the off-axis extra line[61] and the "forbidden" transition with $\Delta m_s=\pm 2$ and ± 3. The parameters used for the simulation are $S=3/2$, $g=2.003$ (isotropic), $D=+0.1350$ cm^{-1}, and $|E|=0.0040$ cm^{-1} for conformer I and $S=3/2$, $g=2.003$ (isotropic), $D=+0.1285$ cm^{-1}, and $|E|=0.0055$ cm^{-1} for conformer II, and the ratio of conformer I to II is 1 : 1. The spectrum at the bottom shows the simulated spectra of conformer I (solid line) and II (dotted line) and the spectrum in the middle is the superposition of the two. The sign of D was determined from the temperature dependence of the ESR spectrum (see the text).

canonical peaks coincide and the corresponding pairs of the X-axis peaks show a doublet structure.[60] These features are in a good agreement with the observed spectrum. Likewise, the other pairs of the X and Y-axis peaks and "forbidden" transitions of $\Delta m_s=\pm 2$ and ± 3 marked by F as well as the off-axis extra lines denoted by A altogether give a satisfactory agreement with the observed spectrum. A discussion on the extra lines will be given below. However, the predicted Z-axis canonical peaks are not seen in the observed spectrum because the low- and the middle-field peaks are masked by the signals of by-produced triplet carbenes and doublet radicals, respectively. The high-field Z-axis peaks also cannot be distinguished from the noise because of their weak intensity. In order to confirm the generation of the two conformers, the high-field Z-axis canonical peaks were disclosed by averaging the signals over 100 scans. The detected spectrum is shown in Fig. 4 where the base-line correction was made and a smoothing was carried out. The spectrum revealed the anticipated doublet feature of the Z-axis peak unequivocally showing the generation of the two conformers. Once the peak positions of the high-field Z-axis canonical peaks are known, the fine structure parameter D can be determined accurately. Since the fine structure parameters of the two conformers are close to each other, the difference of the conformations must be small to rule out a large conformational change such as the cis–trans isomerism. It might be that the two conformers are different in the degree of planarity and/or the bond angles at the divalent carbon atoms. The intensities from the two conformers are nearly equal. The best fit parameters are found as to be $S=3/2$, $g=2.003$ (isotropic), $D=+0.1350$ cm^{-1}, and $|E|=0.0040$ cm^{-1} for conformer I and $S=3/2$, $g=2.003$ (isotropic), $D=+0.1285$ cm^{-1}, and $|E|=0.0055$ cm^{-1} for conformer II. The sign of D was determined from the effect of Boltzmann factor on the relative intensity of ESR transitions (see below). The parameters are found to be close to those of the anion of m-PBPM ($g=2.003$ (isotropic), $D=+0.1200$ cm^{-1}, and $|E|=0.0045$ cm^{-1}).[12]

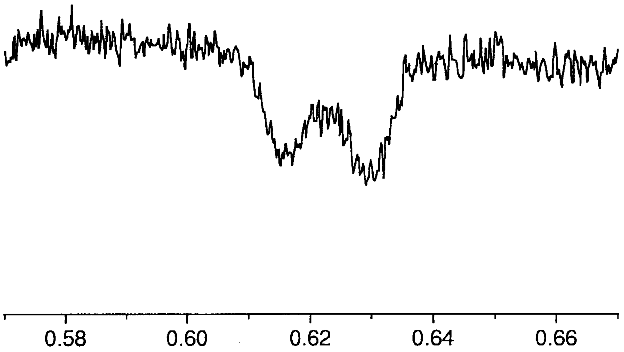

Fig. 4. Observed X-band ESR spectrum around the high-field Z-axis canonical peak of m-PBPM$^{+\bullet}$. The spectrum was obtained by accumulating the signals over 100 scans and carrying out the base-line correction and a suitable smoothing. Microwave frequency is 9.56262 GHz. The doublet structure of the Z-axis peak clearly shows the formation of two conformers of m-PBPM$^{+\bullet}$.

As discussed elsewhere,[61] the off-axis extra lines in the powder-pattern fine-structure spectrum are characteristic of the spin multiplicity as well as the fine structure parameters. In general, the off-axis extra lines of $\Delta m_s=\pm 1$ do not appear for the triplet. They tend to appear with increasing the spin multiplicity and the fine structure energy and with decreasing the microwave frequency. As for the half-integral spin state, however, the off-axis extra lines always occur in the transition between the central Kramers doublet ($m_s=-1/2\leftrightarrow 1/2$).[61] It depends only upon the linewidth-to-D value ratio whether they are resolved in the spectrum and discriminated from ordinary canonical orientations. Fig. 5 shows the calculated angular dependence of the resonant fields and the powder-pattern first derivative ESR spectra for conformers I and II. For both conformers the off-axis extra line denoted by A appears at $\theta_{ex}=37°$ in the transition between the sublevels of $m_s=-1/2$ and 1/2. The appearance of the off-axis extra lines assures that the observed fine structure pattern, indeed, arises from the species with the half-integral spin of 3/2.

At temperatures as low as 1.4 K the relative intensity of ESR transitions in the quartet state should depend sensitively on the thermal population among the sublevels. From the temperature dependence of the intensity ratio of the high-field to the low-field Y-axis peak, the sign of D was determined to be positive because the intensity of transitions between sublevels of the high-field should become weak relative to those of the low-field as the temperature was lowered. Since the relative intensity of the low-field X-axis canonical peak of conformer I to that of conformer II did not change with the temperature, the ground state of both I and II must be the same. The state is quartet as shown in the next section. The same temperature dependence of I and II also implies that the sign of D is the same for the two conformers.

Spin Multiplicity of the Ground State of m-PBPM$^{+\bullet}$. In order to determine the spin multiplicity of the ground state of m-PBPM$^{+\bullet}$, the temperature dependence of the intensity of the quartet signal was examined by monitoring the low-field Y-axis canonical peak (see the spectrum in Fig. 6). The intensity was calculated by double integration of the first derivative peak. For the measurement of the temperature of the sample the neutral m-PBPM was used as an internal standard of the temperature as in the case of the anionic system.[12] In order to get a proper intensity of m-PBPM for the comparison with that of the monocation shown in Fig. 6a, the yield of m-PBPM was controlled by using visible light with $\lambda > 510$ nm instead of UV

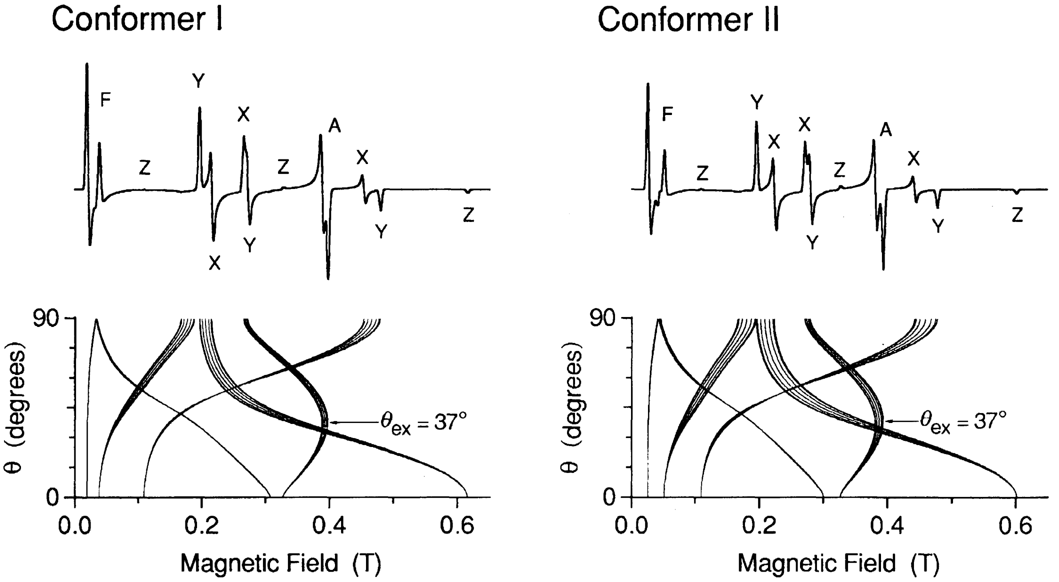

Fig. 5. Calculated angular dependence of resonant field and the powder-pattern first derivative ESR spectra for conformers I and II of *m*-PBPM$^{+\bullet}$. Microwave frequency was set to 9.175 GHz. θ_{ex} denotes the angle corresponding to the extra line. The parameters are $S=3/2$, $g=2.003$ (isotropic), $D=+0.1350$ cm^{-1}, and $|E|=0.0040$ cm^{-1} for conformer I and $S=3/2$, $g=2.003$ (isotropic), $D=+0.1285$ cm^{-1}, and $|E|=0.0055$ cm^{-1} for conformer II.

light. By obtaining both *m*-PBPM and its cation in this way and carefully avoiding the rapid passage effect and the signal saturation by microwave power, the temperature of the sample was calibrated referring to the signal intensity of *m*-PBPM. The observed intensity is represented by circles in Fig. 6b. The approximately linear plot obtained indicates that the ground state of *m*-PBPM$^{+\bullet}$ is quartet.

^{1}H ENDOR Spectra. The neutral *m*-PBPM has four SOMO's, two of which are the non-bonding π-orbitals and the other two are the in-plane n-orbitals localized at the divalent carbon atoms.[3—5] Therefore, there are two possibilities for the cation, that is, a π- or an n-cation as in the case of the anion.[12] In the case of the π-cation, the spin density of the π-orbital is expected to be about one half of that of the neutral *m*-PBPM, whereas it will be almost the same as that of *m*-PBPM for the n-cation because the n-orbitals are nearly localized on the divalent carbons. In order to compare the hfcc of the quartet cation with that of the quintet *m*-PBPM, the difference of the spin multiplicity must be taken into account. According to the projection theorem,[62] the proton hfcc is proportional to $\rho/2S$ where S denotes the total electron spin quantum number of the system studied and ρ is the spin density on the carbon bonded to the α-proton. Therefore, for the π- and n-cation the hfcc of the protons is expected to be 2/3 and 4/3 of those of *m*-PBPM, respectively.

^{1}H ENDOR spectra were measured by monitoring the X-, Y-axis canonical peaks and the off-axis extra line. The ENDOR signals were weaker than those of the monoanion in MTHF[12] and they were obtained only for the three ESR peaks at 202.5, 281.4, and 396.1 mT (see Fig. 3). Since all the three peaks consist of the peaks due to conformers I and II, the observed ENDOR signals are superposition of the signals due to conformer I and conformer II. The weak ENDOR signals were accumulated at 3.0 K over several hundred scans to obtain the spectra shown in Fig. 7. Since the hfcc due to each proton cannot be distinguished, only a semiquantitative discussion can be made as in the case of *m*-PBPM$^{-\bullet}$.[12] Each spectrum is quite similar to the corresponding ^{1}H ENDOR spectrum of the anion. The hfcc's of the protons of the cation should, therefore, be close to those of the anion. The spin density of the π-orbital of the cation is about one half of that of *m*-PBPM as in the case of the anion;[12] The hfcc's of the cation are within 8—10 MHz in all of the observed spectra and most of those are less than 2 MHz. They are about 2/3 of those of *m*-PBPM, which are reported as $a_{\text{iso}}=-8.0$—3.6 MHz and $|a_{\text{aniso}}|\leq 4$ MHz.[63] Thus, it is concluded that the hole in the cation is in the π-orbital.

The close agreement of the hfcc's of the anion and the cation is consistent with the conclusion that both the anion and the cation are of π-type ions, because the pairing theorem[57—59] should hold in alternant π electron systems.[64—66]

The observed ENDOR spectra of Figs. 7a, 7b, and 7c correspond to the orientation of the principal Y-axis, X- and Y-axes ($\theta=90°$), and the direction of the off-axis extra-line[61] ($\theta=37°$), respectively. Although the observed ENDOR spectra are the superposition of the signals due to conformer I and conformer II, the hfcc's in the three different directions agree fairly well with those of the monoanion. Therefore, the orientations of each hfcc tensor of the two conformers should be close to each

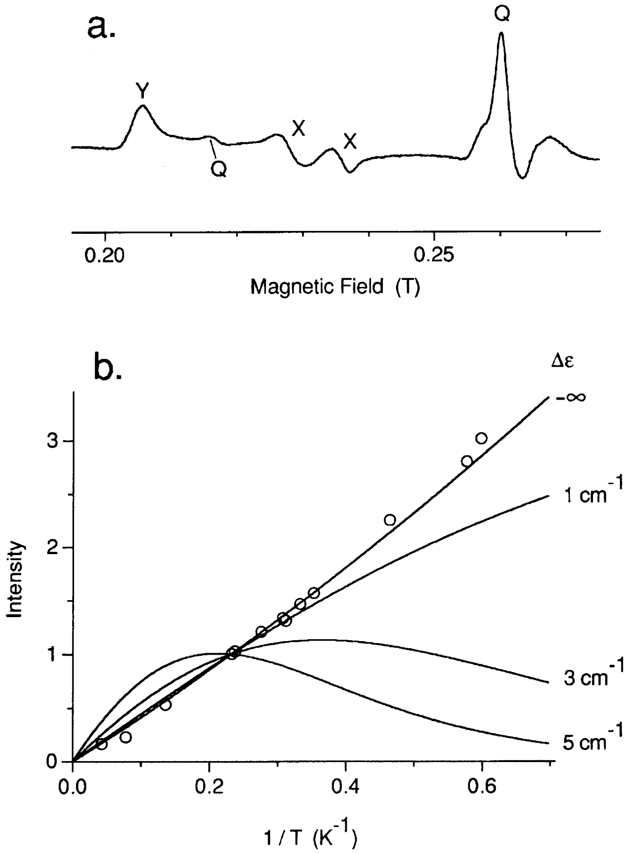

Fig. 6. **a**. Typical ESR spectrum used for the calculation of the temperature dependence of the low-field Y-axis canonical peak of the quartet state. The symbols X and Y indicate the low-field X and Y-axis canonical peaks of the quartet cation. The signals due to the neutral quintet are denoted by Q. The temperature was calibrated by the intensity of the signal of the neutral *m*-PBPM at ≅0.26 T.

b. Temperature dependence of the intensity of the ESR signal of the low-field Y-axis canonical peak. The circles are experimental, and the solid curves are the calculated for several values of $\Delta\varepsilon=\varepsilon(\text{quartet})-\varepsilon(\text{doublet})$. In the calculation for the curve denoted by $\Delta\varepsilon=-\infty$ the population in the doublet state was totally ignored. The curve of $\Delta\varepsilon=-\infty$ corresponds to the case that the ground state is quartet. Thus, from the observed temperature dependence, it is safely concluded that the ground state of *m*-PBPM$^{+\bullet}$ is quartet. All the experimental and theoretical intensities are normalized at T=4.3 K.

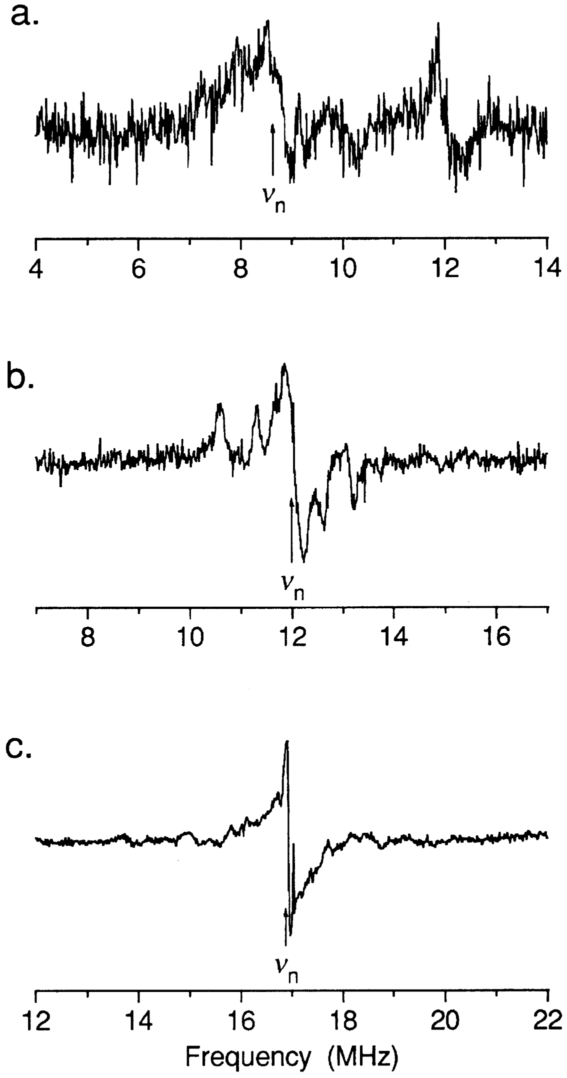

Fig. 7. ^{1}H ENDOR spectra of *m*-PBPM$^{+\bullet}$. The measurements were performed at 3.0 K. The magnetic field employed and the number of scans are as follows. **a**. 202.5 mT (Y-axis canonical peak of the transition from $m_S=-3/2$ to $-1/2$ sublevels) with 530 scans. **b**. 281.4 mT (X-and Y-axis canonical peaks of the transition from $m_S=-1/2$ to $1/2$ sublevels) with 337 scans. **c**. 396.1 mT (extra-line of the transition from $m_S=-1/2$ to $1/2$ sublevels) with 340 scans.

other and also close to that of the monoanion. Thus, we can expect that the conformations of the two conformers of the cation and that of the anion are similar. Then, the fine structure parameters of the cation should be close to those of the anion, which was indeed observed. The conformation of the cation will be discussed further in a later section.

ESR Spectra of the ^{13}C Isotopomer. If the hole of the cation resides on the singly-occupied π-orbital, the spin density of the two n-orbitals must be essentially the same as that in *m*-PBPM and the isotropic hfcc's of the two divalent carbon atoms are approximately equal. In order to ensure the assignment of the π-cation, we examined a ^{13}C-labeled isotopomer in which one of the two divalent carbon atoms is substituted by ^{13}C. Figure 8 compares the low-field Y- and X-axis canonical peaks of the ^{13}C isotopomer with those of the ^{12}C isotopomer. Each peak of the ^{13}C isotopomer is broadened by the unresolved hyperfine splitting due to ^{13}C. The broad bell-shaped peak of the ^{13}C isotopomer indicates that the hfcc's of the two ^{13}C atoms are approximately equal.[12] If the hole occupied the localized n-orbital, the

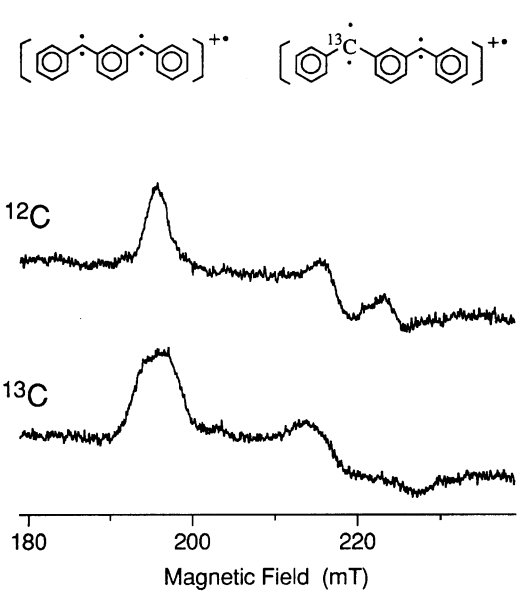

Fig. 8. The ESR spectrum of ^{13}C substituted *m*-PBPM$^{+\cdot}$ in which one of the two divalent carbon atoms was substituted by ^{13}C. The spectrum of ^{12}C isotopomer is also shown for comparison.

spin density of one of the two n-orbitals should vanish and the hfcc of that carbon atom must be small whereas the other carbon atom should have essentially the same hfcc as that of the neutral *m*-PBPM, 3.5 mT,[67] except for the difference of the spin projection factor $1/2S$. The superposition of the two components expected from the n-cation never reproduced the unresolved bell-shaped peak which was observed.[12] Thus, the ESR spectrum of ^{13}C isotopomer indicates that the hole of the cation is in the π-orbital, which is consistent with the result of ^{1}H ENDOR measurements described above.

We attempted to observe the ^{13}C ENDOR spectrum to determine the hfcc of ^{13}C, but we failed to detect the signal because of low signal-to-noise ratios.

Conformation of *m*-PBPM$^{+\cdot}$. The fine structure tensor of aromatic polycarbenes can be represented approximately as a superposition of the one center spin–spin interaction of n-π type at each divalent carbon atom.[21,24,25,68,69] Therefore, the fine structure tensor is determined mainly by the relative orientation of the one-center interaction tensors and the spin density at the divalent carbon atoms. Since the fine structure parameters and the electronic structure of the cation are now determined, we can derive the conformation of the cation by considering the relative orientation of the one-center interaction tensors. Since they can be approximated by the fine structure tensor of diphenylmethylene (DPM), the semiquantitative expression for the fine structure tensor is given as follows.[24,25]

$$D_{ij} = [S(2S-1)]^{-1}\sum_{k}(\rho_k/\rho_{\mathrm{DPM}})(\boldsymbol{U}_k\cdot\boldsymbol{D}_{\mathrm{DPM}}\cdot\boldsymbol{U}_k{}^{-1})_{ij},\quad i,j = X,Y,Z, \tag{6}$$

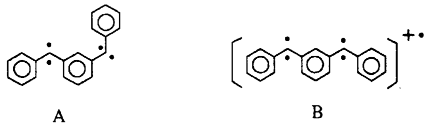

A B

Chart 1.

where the subscript k runs over all the divalent carbon atoms and $\boldsymbol{D}_{\mathrm{DPM}}$ denotes the fine structure tensor of DPM represented in the principal axis system. The symbols ρ_k and ρ_{DPM} represent the spin density of the π-electron at the *k*th divalent carbon atom of the high-spin system under study and that at the divalent carbon atom of DPM, respectively. The unitary matrix $\boldsymbol{U}_k$ transforms the molecule fixed axes to the principal axes of the one center interaction tensor at *k*th divalent atom. Since a simple LCAO–MO calculation gives the spin densities of $\rho_{\mathrm{DPM}}=2/5$ and $\rho_{m\text{-PBPM}}=0.4040$, the ratio $\rho_{m\text{-PBPM}}/\rho_{\mathrm{DPM}}$ can be regarded as unity.[21,24,25] Table 1 compares the fine structure parameters of the monoions with those of DPM[70] and *m*-PBPM.[5] If the conformation of the cation was the same as that of the neutral *m*-PBPM which is known to be a cis-trans type as shown in Conformation A,[5,63] the fine structure tensor of the cation would be approximately equal to that of *m*-PBPM, because in the π-cation the π-electron density is expected to be halved but the projection factor $[S(2S-1)]^{-1}$ for the cation should be doubled against the quintet *m*-PBPM (the factor is 1/3 for the quartet and 1/6 for the quintet). On the other hand, when the conformation of the cation is of a trans-trans type where the two one-center interaction tensors are roughly parallel, the fine structure parameters are estimated as 1/3 of those of DPM, because the sum in Eq. 6 $\sum_k(\rho_k/\rho_{\mathrm{DPM}})(\boldsymbol{U}_k\cdot\boldsymbol{D}_{\mathrm{DPM}}\cdot\boldsymbol{U}_k^{-1})_{ij}$ is approximately equal to $\boldsymbol{D}_{\mathrm{DPM}}$ and the projection factor $[S(2S-1)]^{-1}$ is 1/3 for the quartet and 1 for the triplet DPM. The experimentally determined values for both of the two conformers are closer to the latter value of $D_{\mathrm{DPM}}/3=+0.135$ cm^{-1} and $|E_{\mathrm{DPM}}|/3=0.0064$ cm^{-1} (see Table 1). The $|E/D|$ ratio, which is a measure of the deviation from the axial symmetry of the tensor, also supports the latter case; the ratio is 0.030 for conformer I and 0.043 for conformer II and they are close to that of DPM, 0.04735,[70] but far from that of *m*-PBPM, 0.2667[5] (see Table 1). Table 1 includes the fine structure parameters and the $|E/D|$ ratio for a trans-trans type of *m*-PBPM which have been obtained by a semiempirical calculation based on Eq. 6 assuming the bond angle of the divalent carbon atom.[71] These calculated values also support the above argument. Thus, the conformation of the cation is plausibly in a trans-trans type as indicated by Conformation B (Chart 1).

The value of $(2S-1)D$ in Table 1 is a useful measure of the spin–spin interaction in organic high-spin molecules, providing us with the magnitude and type of the interaction as well as their important molecu-

Table 1. Comparison of D, $|E|$, $|E/D|$, and $(2S-1)D$ of Monoions of *m*-Phenylenebis(phenylmethylene) (*m*-PBPM) with Those of Diphenylmethylene and the Neutral *m*-PBPM

	S	D / cm^{-1}	$\lvert E\rvert$ / cm^{-1}	$\lvert E/D\rvert$	$(2S-1)D$ / cm^{-1}	Reference
Monocation of *m*-PBPM conformer I	3/2	+0.1350	0.0040	0.030	+0.2700	This work
ditto conformer II	3/2	+0.1285	0.0055	0.043	+0.2570	This work
Monoanion of *m*-PBPM	3/2	+0.1200	0.0045	0.038	+0.2400	11,12
Diphenylmethylene	1	+0.40505	0.01918	0.04735	+0.40505	70
m-Phenylenebis(phenylmethylene)(*m*-PBPM) *cis−trans*	2	+0.07131	0.01902	0.2667	+0.21393	5
ditto *cis−trans*	2	+0.08192	0.02408	0.294	+0.24576	Calculated
ditto *trans−trans*	2	+0.1292	0.00833	0.0645	+0.3876	Calculated

lar structural information.[4,24—26] This holds not only for similar systems studied here but also for high-spin systems characterized by π-π types of the interaction such as triphenylmethyl radical based high-spin systems.[31—35,47] The high-spin molecules ($S>1$) listed in Table 1 have a similar molecular structure of the trans-trans type to that depicted as Conformation B except for the cis-trans *m*-PBPM. A nearly 50% reduction of the $(2S-1)D$ value occurs in the cis-trans *m*-PBPM relative to that in DPM. The reduction is responsible for the asymmetry of the molecular structure of the cis-trans form, where the tensorial contribution of the two local constituent fine structure tensors is not completely additive but cancelled a great deal. If *m*-PBPM has a molecular structure with C_2 symmetry such as a trans-trans form, only a small amount of the cancellation takes place due to the larger bond angle of the divalent carbon atom than 120° (see the calculated value of the trans-trans *m*-PBPM in Table 1). As a result, the trans-trans *m*-PBPM has a $(2S-1)D$ value close to $0.40505\ \mathrm{cm}^{-1}$ for DPM, indicating that the type and magnitude of the spin-spin interaction in *m*-PBPM are essentially the same as in DPM.

The remarkable reduction of the $(2S-1)D$ value for the high-spin ions of *m*-PBPM, that is, a nearly 40% reduction for the monoanion and 32% for the monocation, respectively, relative to DPM and the trans-trans *m*-PBPM, is attributed to the electron configuration in the topologically degenerate two π nonbonding orbitals, i.e., three π-electrons occupying the two π nonbonding orbitals for the monoanion and a single π-electron occupying them for the monocation. Both the electron configurations reduce the π spin density on the divalent carbons by nearly 50%, resulting in the corresponding amount of the reduction in the spin–spin interaction in the case of the dominant n-π one-center interaction. This is the case for the anion and cation of *m*-PBPM. Thus, the major cause for the reduction of the $(2S-1)D$ value in the ions of *m*-PBPM is concluded to arise from the change in electron configuration in the degenerate π nonbonding orbitals and the asymmetry of their molecular structure is not a dominant contribution.

Conclusion

We have detected for the first time a positively charged high-spin hydrocarbon molecule and have shown that the ground state of $m\text{-PBPM}^{+\bullet}$ is quartet. The result is similar to the anion of $m\text{-PBPM}^{-\bullet}$, whose ground state is also quartet.[12] A suggestion of the possible reversal of the order of spin states upon charging[49,50] was not substantiated in both the monocation and the monoanion of *m*-PBPM. From the ^{1}H ENDOR measurements the hole and the excess electron in the cation and the anion, respectively, are found to reside in the nonbonding π-orbital. The fine structure parameters and the electronic structure obtained indicate that the conformations of the ions are in a trans-trans conformation in contrast to the cis-trans conformation of the neutral quintet *m*-PBPM.[5,63] The result of the present study, together with that of the previous study on the ainonic system, is important for elucidating the relation between the excess charge and the spin alignment in topologically controlled π-conjugated high-spin systems. In order to clarify the difference between electron attachment and removal in such systems and to make a more detailed discussion on the electronic structure of charged high-spin systems, experimental and theoretical studies of smaller π-conjugated systems are now in progress.

The Kyoto group is indebted to Professor Takashi Kawamura for allowing us to use the facilities of his laboratory. The Osaka group thanks both the Computer Center, Institute for Molecular Science, Okazaki National Research Institutes for the use of the HITAC M680H computer and the Computer Center, Osaka City University. Spectral simulations were also carried out at the Data Processing Center of Kyoto University. The study was partially supported by Grants-in-Aid for Scientific Research on Priority Areas (Grant Nos. 02205070, 02205102, and 04242103), Grant-in-Aid for General Scientific Research (Grant Nos. 02453014 and 03640429) and Grants-in-Aid for Scientific Research on Priority Areas "Molecular Magnetism" (Area No. 228) from the Ministry of Education, Science and Culture.

References

1) S. Morimoto, F. Tanaka, K. Itoh, and N. Mataga, "Preprint of Symposium on Molecular Structure," 67 (1968).

2) N. Mataga, *Theor. Chim. Acta*, **10**, 372 (1968).

3) K. Itoh, *Bussei*, **12**, 635 (1971).

4) K. Itoh, *Pure Appl. Chem.*, **50**, 1251 (1978).

5) K. Itoh, *Chem. Phys. Lett.*, **1**, 235 (1967).

6) E. Wasserman, R. W. Murray, W. A. Yager, A. M. Trozzolo, and G. Smolinsky, *J. Am. Chem. Soc.*, **89**, 5076 (1967).

7) E. Wasserman, K. Schueller, and W. A. Yager, *Chem. Phys. Lett.*, **2**, 259 (1968).

8) "Proceedings of the Symposium on Ferromagnetic and High-Spin Molecular Based Material," at "197th National Meeting of the American Chemical Society," Dallas, TX, April, 1989; J. S. Miller and D. A. Dougherty, *Mol. Cryst. Liq. Cryst.*, **176**, 1-562 (1989).

9) "Materials Research Society Symposium Proceedings," Materials Research Society, Boston, M. A., 1989 Fall Meeting, Vol. 173; "Advanced Organic Solid State Materials," ed by L. Y. Chiang, P. M. Chaikin, and D. O. Cowan, Materials Research Society, Pittsburgh, Pennsylvania (1989), p. 3-92.

10) "Proceedings of the NATO Advanced Research Workshop on Molecular Magnetic Materials," "II Ciocco," ed by Castelevecchio Pascoli, Lucca, Italy; "Molecular Magnetic Materials," ed by D. Gatteschi, O. Kahn, J. S. Miller, and F. Palacio, Kluwer Academic, Dordrecht (1991), Vol. A198.

11) M. Matsushita, T. Momose, T. Shida, Y. Teki, T. Takui, and K. Itoh, *J. Am. Chem. Soc.*, **112**, 4700 (1990).

12) M. Matsushita, T. Nakamura, T. Momose, T. Shida, Y. Teki, T. Takui, T. Kinoshita, and K. Itoh, *J. Am. Chem. Soc.*, **114**, 7470 (1992).

13) A. A. Ovchinnikov, *Theor. Chim. Acta*, **47**, 297 (1978).

14) D. J. Klein, C. J. Nelin, S. Alexander, and F. A. Matsen, *J. Chem. Phys.*, **77**, 3101 (1982).

15) Y. Teki, T. Takui, T. Kinoshita, S. Ichikawa, H. Yagi, and K. Itoh, *Chem. Phys. Lett.*, **141**, 201 (1987).

16) Y. Teki, T. Takui, M. Kitano, and K. Itoh, *Chem. Phys. Lett.*, **142**, 181 (1987).

17) S. A. Alexander and D. J. Klein, *J. Am. Chem. Soc.*, **110**, 3401 (1988).

18) K. Itoh, T. Takui, Y. Teki, and T. Kinoshita, *J. Mol. Electron.*, **4**, 181 (1988).

19) K. Itoh, T. Takui, Y. Teki, and T. Kinoshita, *Mol. Cryst. Liq. Cryst.*, **176**, 49 (1989).

20) T. Takui and K. Itoh, *Chem. Phys. Lett.*, **19**, 120 (1973).

21) T. Takui, Dr. Thesis, Osaka University, 1973.

22) Y. Teki, T. Takui, H. Yagi, K. Itoh, and H. Iwamura, *J. Chem. Phys.*, **83**, 539 (1985).

23) Y. Teki, T. Takui, K. Itoh, H. Iwamura, and K. Kobayashi, *J. Am. Chem. Soc.*, **105**, 3722 (1983).

24) Y. Teki, T. Takui, K. Itoh, H. Iwamura, and K. Kobayashi, *J. Am. Chem. Soc.*, **108**, 2147 (1986).

25) Y. Teki, Dr. Thesis, Osaka City University, 1986.

26) I. Fujita, Y. Teki, T. Takui, T. Kinoshita, K. Itoh, F. Miko, Y. Sawaki, H. Iwamura, A. Izuoka, and T. Sugawara, *J. Am. Chem. Soc.*, **112**, 4074 (1990).

27) K. Reibisch, G. Kothe, and J. Brickmann, *Chem. Phys. Lett.*, **17**, 86 (1972).

28) J. Brickmann and G. Kothe, *J. Chem. Phys.*, **59**, 2807 (1973).

29) D. A. Kaisaki, W. Chang, and D. A. Dougherty, *J. Am. Chem. Soc.*, **113**, 2764 (1991).

30) D. A. Dougherty, *Acc. Chem. Res.*, **24**, 88 (1991).

31) A. Rajca, *J. Am. Chem. Soc.*, **112**, 5889 (1990).

32) A. Rajca, *J. Am. Chem. Soc.*, **112**, 5890 (1990).

33) A. Rajca, S. Utampanya, and J. Xu, *J. Am. Chem. Soc.*, **113**, 9235 (1991).

34) S. Utampanya and A. Rajca, *J. Am. Chem. Soc.*, **113**, 9242 (1991).

35) A. Rajca, S. Utampanya, and S. Thayumanavan, *J. Am. Chem. Soc.*, **114**, 1884 (1992).

36) T. Ishida and H. Iwamura, *J. Am. Chem. Soc.*, **113**, 4328 (1991).

37) K. Inoue, N. Koga, and H. Iwamura, *J. Am. Chem. Soc.*, **113**, 9803 (1991).

38) N.Nakamura, K. Inoue, H. Iwamura, T. Fujioka, and Y. Sawaki, *J. Am. Chem. Soc.*, **114**, 1484 (1992).

39) M. Kinoshita, P. Turek, M. Tamura, K. Nozawa, D. Shiomi, Y. Nakazawa, M. Ishikawa, M. Takahashi, K. Awaga, T. Inabe, and Y. Maruyama, *Chem. Lett.*, **1991**, 1255.

40) M. Takahashi, P. Turek, Y. Nakazawa, M. Tamura, K. Nozawa, D. Shiomi, M. Ishikawa, and M. Kinoshita, *Phys. Rev. Lett.*, **67**, 746 (1991).

41) P. M. Allemand, K. C. Khemani, A. Koch, F. Wudl, K. Holczer, S. Donovan, G. Grüner, and J. D. Thompson, *Science*, **253**, 301 (1991).

42) C. Kollmer and O. Kahn, *J. Am. Chem. Soc.*, **113**, 7987 (1991).

43) C. Kollmar, M. Couty, and O. Kahn, *J. Am. Chem. Soc.*, **113**, 7994 (1991).

44) W. E. Broderick, J. A. Tohompson, E. P. Day, and B. M. Hoffman, *Science*, **249**, 401 (1990).

45) J. M. Manriquez, G. T. Yee, R. S. McLean, A. J. Epstein, and J. S. Miller, *Science*, **252**, 1415 (1991).

46) G. T. Yee, J. M. Manriquez, D. A. Dixon, R. S. McLean, D. M. Groski, R. B. Flippen, K. S. Narayan, R. S. Epstein, and J. S. Miller, *Adv. Mater.*, **3**, 309 (1991).

47) J. Veciana, C. Rovira, M. I. Crespo, O. Armet, V. M. Domingo, and F. Palacio, *J. Am. Chem. Soc.*, **113**, 2552 (1991).

48) P. M. Lahti, A. S. Ichimura, *J. Org. Chem.*, **56**, 3030 (1991).

49) K. Yamaguchi, Y. Toyoda, and T. Fueno, *Synth. Met.*, **19**, 81 (1987).

50) K. Yamaguchi et al., personal communication. Very recently Yamaguchi's group of Osaka University has carried out more sophisticated MO calculations of various levels of approximation in order to reproduce our experimental results. The calculated results are consistent with the experimental ones, but the calculation predicts that some simple π conjugated molecules favor the low-spin ground state upon charging.

51) S. -I. Murahashi, Y. Yoshimura, Y. Yamamoto, and I. Moritani, *Tetrahedron*, **4**, 1485 (1972).

52) 1,3-BDB was obtained by oxidizing the corresponding hydrazone with activated MnO_2 in stead of HgO.

53) T. Shida, E. Haselbach, and T. Bally, *Acc. Chem. Res.*, **17**, 180 (1984).

54) T. Shida, "Electronic Absorption Spectra of Radical Ions," "Physical Sciences Data 34," Elsevier Science Publishers, Amsterdam (1988), p. 446.

55) T. Shida, *Annu. Rev. Phys. Chem.*, **42**, 55 (1991).

56) K. Itoh, H. Konishi, and N. Mataga, *J. Chem. Phys.*, **48**, 4789 (1968).

57) A. D. McLachlan, *Mol. Phys.*, **2**, 271 (1959).

58) A. D. McLachlan, *Mol. Phys.*, **4**, 49 (1961).

59) J. Koutecký, *J. Chem. Phys.*, **44**, 3702 (1966).

60) For the sake of convenience the principal-axis transitions X and Y are labeled under the assumption of $E>0$.

61) Y. Teki, T. Takui, and K. Itoh, *J. Chem. Phys.*, **88**, 6134 (1988).

62) M. E. Rose, "Elementary Theory of Angular Momentum," John Wiley & Sons, New York (1957).

63) T. Takui, S. Kita, S. Ichikawa, Y. Teki, T. Kinoshita, and K. Itoh, *Mol. Cryst. Liq. Cryst.*, **176**, 67 (1989).

64) S. I. Weissman, E. de Boer, and J. J. Conradi, *J. Chem. Phys.*, **26**, 963 (1957).

65) E. de Boer and S. I. Weissman, *J. Am. Chem. Soc.*, **80**, 4549 (1958).

66) A. Carrington, F. Dravnieks, and M. C. R. Symons, *J. Chem. Soc.*, **1959**, 947.

67) Y. Teki et al. to be published.

68) J. Higuchi, *J. Chem. Phys.*, **38**, 1237 (1963).

69) J. Higuchi, *J. Chem. Phys.*, **39**, 1847 (1963).

70) R. W. Brandon, G. L. Closs, C. E. Davoust, C. A. Hutchison, B. E. Kohler, and R. Silbey, *J. Chem. Phys.*, **43**, 2006 (1965).

71) T. Takui et al. unpublished work.